Hindawi Publishing Corporation
Shock and Vibration
Volume 2016, Article ID 5010521, 11 pages
http://dx.doi.org/10.1155/2016/5010521

Research Article

Crash-Induced Vibration and Safety Assessment of Breakaway-Type Post Structures Made of High Anticorrosion Steels

Sang-Youl Lee

Department of Civil Engineering, Andong National University, Andong-si, Gyeongsangbuk-do 760-749, Republic of Korea

Correspondence should be addressed to Sang-Youl Lee; lsy@anu.ac.kr

Received 24 November 2015; Accepted 23 February 2016

Academic Editor: Chao Tao

This study deals with car crash effects and passenger safety assessment of post structures with breakaway types using high performance steel materials. To disperse the impact force when a car crashes into a post, the post could be designed with a breakaway feature. In this study, we used a new high anticorrosion steel for the development of advanced breakaways. Based on the improved Cowper-Symonds model, specific physical properties to the high anticorrosion steel were determined. In particular, the complex mechanism of breakaways was studied using various parameters. The parametric studies are focused on the various effects of car crash on the structural performance and passenger safety of breakaway-type posts. The combined effects of using different steel materials on the dynamic behavers are also investigated.

1. Introduction

Street lights or signboard posts, which are standard roadside structures, are essential elements for the safe passage of vehicles and pedestrians. These facilities are designed to withstand wind loads because of their function as auxiliary roadside structures. However, in terms of automobile crashes, they are hazardous elements on the road.

In sites where there are no guard rails on the roadside, a crash into such a post will cause the vehicle to absorb much of the impact energy, significantly endangering the passengers of the cars. To avoid this problem, a recent study conducted in Korea assessed passenger safety for coupled, rounded posts. A variety of researches in the car crashes or impacts have been performed in the last two decades [1–7]. However, the kinetic examination on the breakaway of the posts subjected to car crashes has not been sufficiently investigated. Recently, techniques for considering strain rate effects are evolved. Choung et al. [8] studied dynamic hardening behaviors of various marine structural steels considering dependencies on strain rate and temperature. In general, the material data obtained from the real high-velocity tensile test can describe accurately the nonlinearity of dynamic behavior. However, it requires high expenses and trial-and-error efforts for the complicated experimental setup. On the other hand, the dynamic approach based on Cowper-Symonds model [9] is free from such requirements and thus can yield more efficient results for high strain rate effects than those of the direct high-velocity tensile test [10]. This allows for convenient use of Cowper-Symonds model. Many Cowper-Symonds theories exist but they are mostly applicable to existing steel structures or rigid jointed posts at the present time.

In this study, we perform a simulation with high anticorrosion breakaway posts capable of absorbing impacts and calculated the breakage stress to assess passenger safety. Passenger safety was assessed by calculating the THIV (Theoretical Head Impact Velocity) and PHD (Post-Impact Head Deceleration) [11]. This process compares normal steel materials (SS400) and high anticorrosion steel materials (SM490). In order to endow specific physical properties to these materials, we used an improved version of the Cowper-Symonds model. The final goal of this study is to assess passenger safety in a car impacting the post. For passenger safety assessment, the THIV requirement is 33 km/h or lower, while the PHD requirement is 20 or less to ensure safety of the passenger. For this reason, we use a coupled breakaway

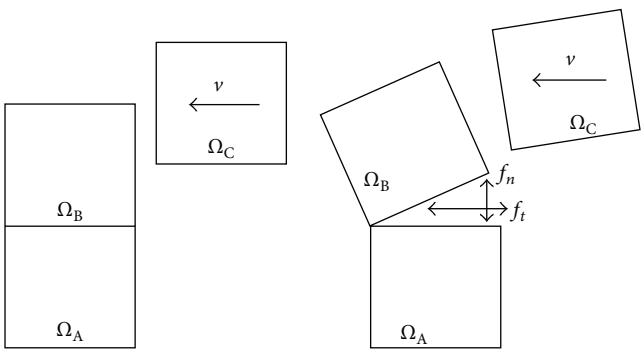

Figure 1: Detachment of the blocks due to impact.

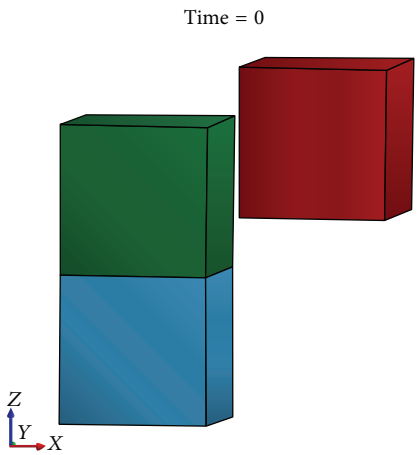

Figure 2: Block impact under full contact conditions (0.0 sec).

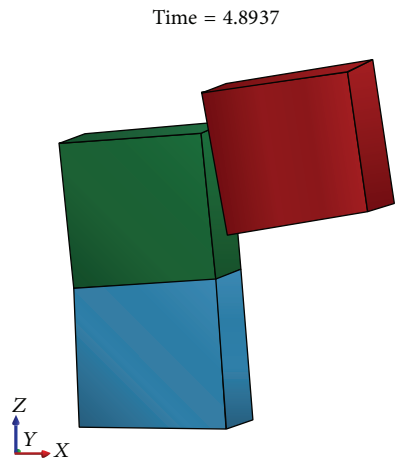

Figure 3: Block impact under full contact conditions (4.8 sec).

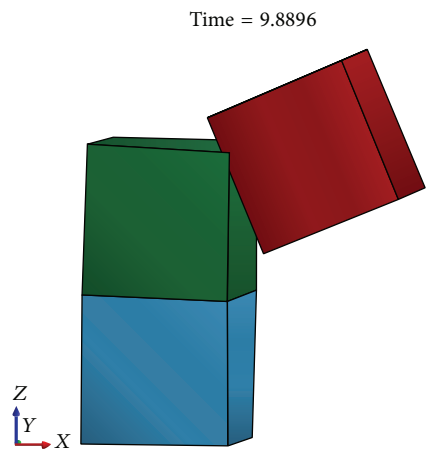

Figure 4: Block impact under full contact conditions (9.8 sec).

post modeling to assess the risks to which passengers are exposed. The focus is on car crash-induced vibration effects for different material properties of breakaway posts. To obtain the results coupled with complicated high strain rate effects, this study uses the modified Cowper-Symonds formulation.

2. Theoretical Formulation

For completeness, the mechanical behaviors and the relevant formulas in the finite element crash analysis using LS-DYNA are reviewed below [10, 12]. If two blocks, namely, Ω_A and Ω_B, collide with block element Ω_C at a velocity of v, the process is as shown in Figure 1. Assuming that blocks Ω_A and Ω_B are completely attached without any gaps, the force at the interface generated in the finite elements after the crash into block Ω_C can be divided into the vertical force f_n and the shearing force f_t. In normal crash interpretations, the vertical force is higher than the shearing force. Especially when one considers an impact breakaway, the vertical force created inside the finite element occurs at the interface due to the momentum of the post.

To represent the mechanical concepts, we use LS-DYNA and the TIEDBREAK_NODES_ONLY option to simulate the distribution of the force on the surface of block Ω_A in a full contact (Figures 2–4). The bottom of block Ω_A is fixed, and blocks Ω_A and Ω_B are assumed to be in complete contact. Block Ω_C proceeds in the x-direction at 0.1 m/s to crash into block Ω_B. Figure 5 shows distributions of the vertical and shearing force in block element Ω_A. In this simulation, simple block models are used and the point of impact is lower than the center of gravity. This is due to the shearing force to become higher. Concerning the post, it is the vertical force that affects the breakaway most significantly. Therefore, in this study the influence from the shearing force is ignored. The maximum vertical force is 2.1 N at 3.83 seconds, and the impact breakaway under the following conditions is applied. For this reason, among the LS-DYNA input TIEDBREAK_NODES_ONLY options NFLF (normal failure force) is 1.0 N, while SFLF (shear failure force) is 1.0 $\times 10^6$ N. Consider

$$f_n < f_n - \max = 2.1\,\text{N}\,(\text{Maximum normal force})\,. \quad (1)$$

Figures 6-7 show the behavior of the blocks after the impact when the vertical force breakaway conditions are applied as set forth above. Figure 8 shows the distribution of the shearing stress in the block Ω_A element. All vertical forces are within the range of 1.0 N. This provides us with a clue that

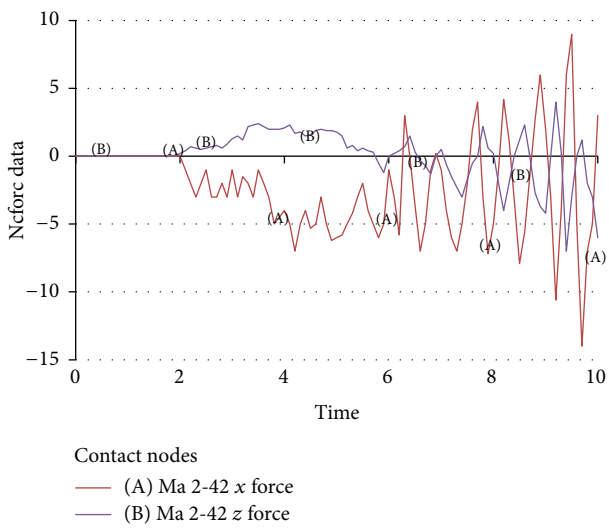

Figure 5: Distributions of the vertical and shearing force in block element Ω_A (z-axis: vertical force, x-axis: shearing force).

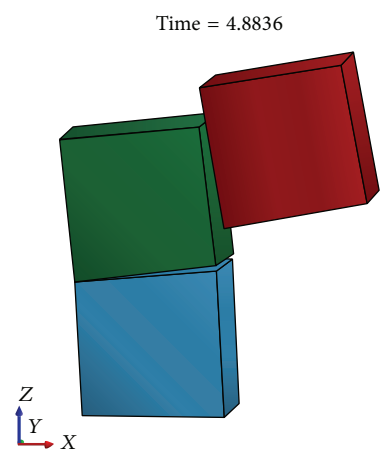

Figure 6: Block impact under breakaway conditions in (1) (4.8 sec).

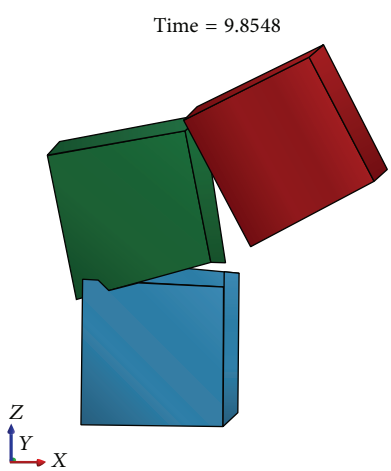

Figure 7: Block impact under the breakaway conditions in (1) (9.8 sec).

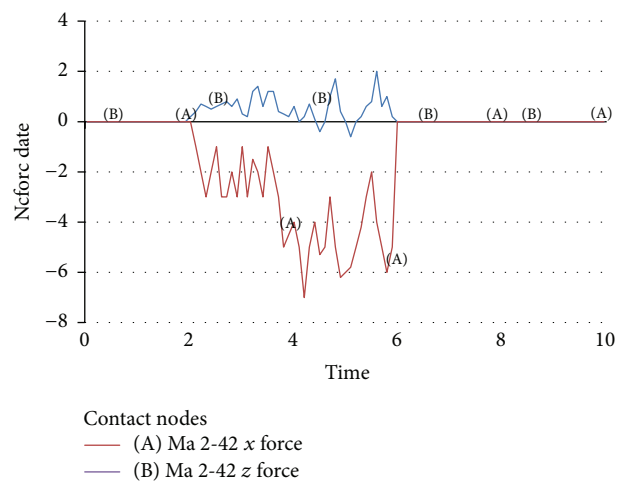

Figure 8: Distributions of the vertical and shearing force in block element Ω_A in consideration of the breakaway conditions (z-axis: vertical force, x-axis: shearing force).

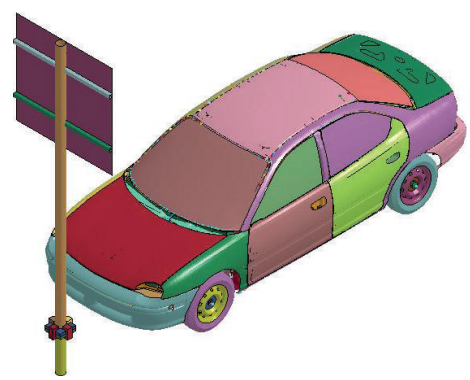

Figure 9: Breakaway-type post model using shell and solid elements.

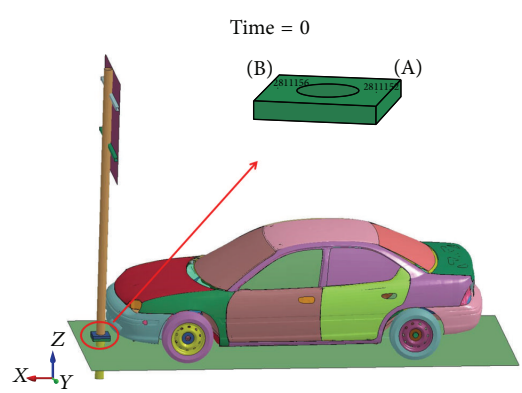

Figure 10: Measuring points of the failure force at the base of the post.

the maximum vertical force is calculated under full contact when the blocks are detached. A failure force of smaller value causes the detachment of the elements.

3. Finite Element Crash Model

The breakaway post is deformed when a car crashes into it. It is designed to break away when the threshold stress value

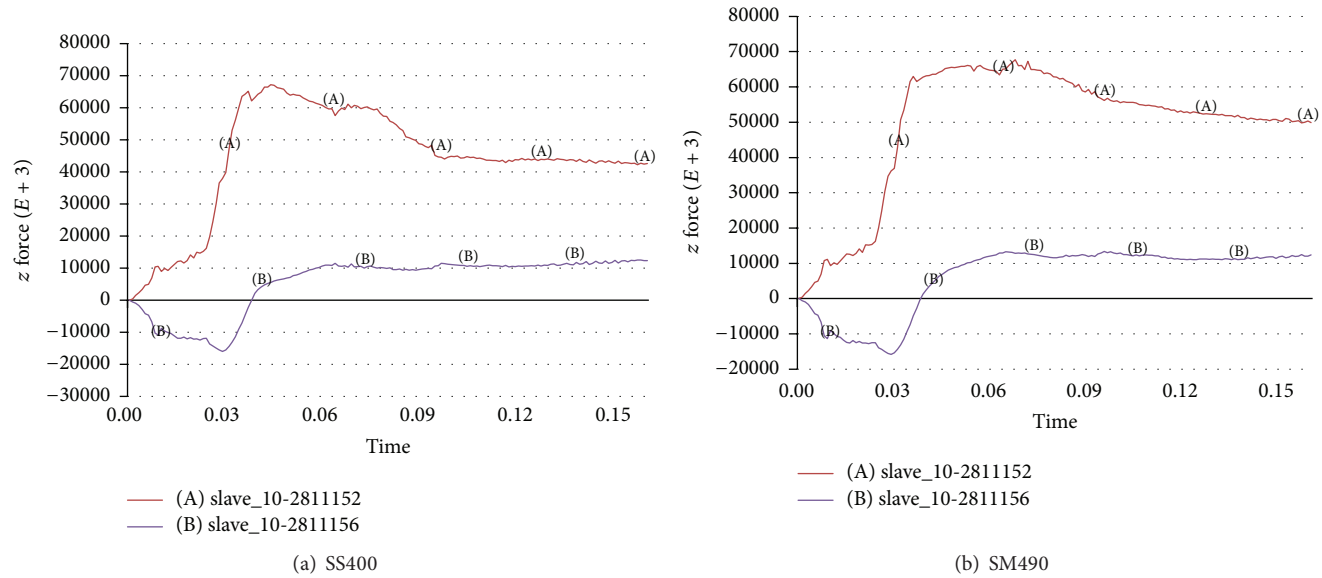

Figure 11: Induced vertical forces in the z-axis at the point of failure force measurement for the full contact condition.

is exceeded during impact. The finite element formulation described earlier is now implemented to compare the results of our technique with those obtained for different material properties and also to study the influences of breakaway on the crash analysis of post structures. In the finite element crash model, the height of the post used for this study is 3,200 mm for the upper post and 500 mm for the lower post, totaling 3,700 mm. The lower post is buried under the ground and modeled to be coupled but with freedom in six directions as shown in Figure 9 [13]. It is also assumed that there is a signboard that is 1,250 mm × 1,200 mm and completely attached to the post. The upper and lower posts are modeled to break away once the threshold failure force is reached. The steel pipe post modeled has a diameter of 101.6 mm and a wall thickness of 4.0 mm using a shell element. The same parameters are given to the signboard, which is modeled as a shell element with 4.0 mm wall thickness. On the other hand, the four facing clips and two slip bases are built in solid elements.

Since the purpose of this study is to compare the safety of passengers with posts built with SS400 and those built with SM490, each of these materials is applied to the post and the results are compared. The material model is based on the Cowper-Symonds equation, with a view to consider the dynamic effect of the vehicle.

In this study, a Dodge Neon is chosen for the passenger vehicle model as provided by NCAC [14], the National Crash Analysis Center of the United States. The physical properties of most of the elements in the vehicle are yield stress of 400 MPa and elastic modulus of 210,000 MPa. The impact interactions between the post and vehicle are limited by the contact options in the LS-DYNA software. In the simulation in this study, the following crash conditions options are also used:

(i) Automatic_single_surface: it removes the domain overlapping effect when there is a crash to enhance the accuracy of the results. This option was applied only to the vehicle model.

(ii) Automatic_surface_to_surface: it endows the contact conditions between the post and vehicle and the post and auxiliary elements.

(iii) Tied_surface_to_surface_failure: it endows the contact conditions between the detached posts. This option requires the maximum vertical stress and shearing stress at the time of the breakaway. This is endowed by $f_{t\text{-max}}$, which is calculated in advance.

The crash simulation in LS-DYNA begins basically with the explicit time interpretation. In case of the explicit analysis, there is a problem that the user has to define an arbitrary time span. For example, narrower spans produce lower accuracy results. In this simulation, we use the automatic time increment option supported by LS-DYNA, because the contact conditions are very complicated. In the numerical test, a total of eighteen cases are simulated. Of these, nine have the posts built with SS400, while the rest had the posts built with SM490. We assumed the wall thickness of the posts to be the same to determine the conditions of breakaway by material.

4. Numerical Examples

4.1. Case I: Full Contacted Posts. Before analyzing breakaway-type posts, we perform crash analyses of the posts under full contact conditions. As mentioned earlier, it is necessary to identify the failure force at the point of breakage under full contact conditions to determine the breakaway load. This is done by the analysis of the full contact case. As shown in Figure 10, the failure force is measured in two positions at the base of the post (A node: 2,811,152 nodes, B node: 2,811,156 nodes).

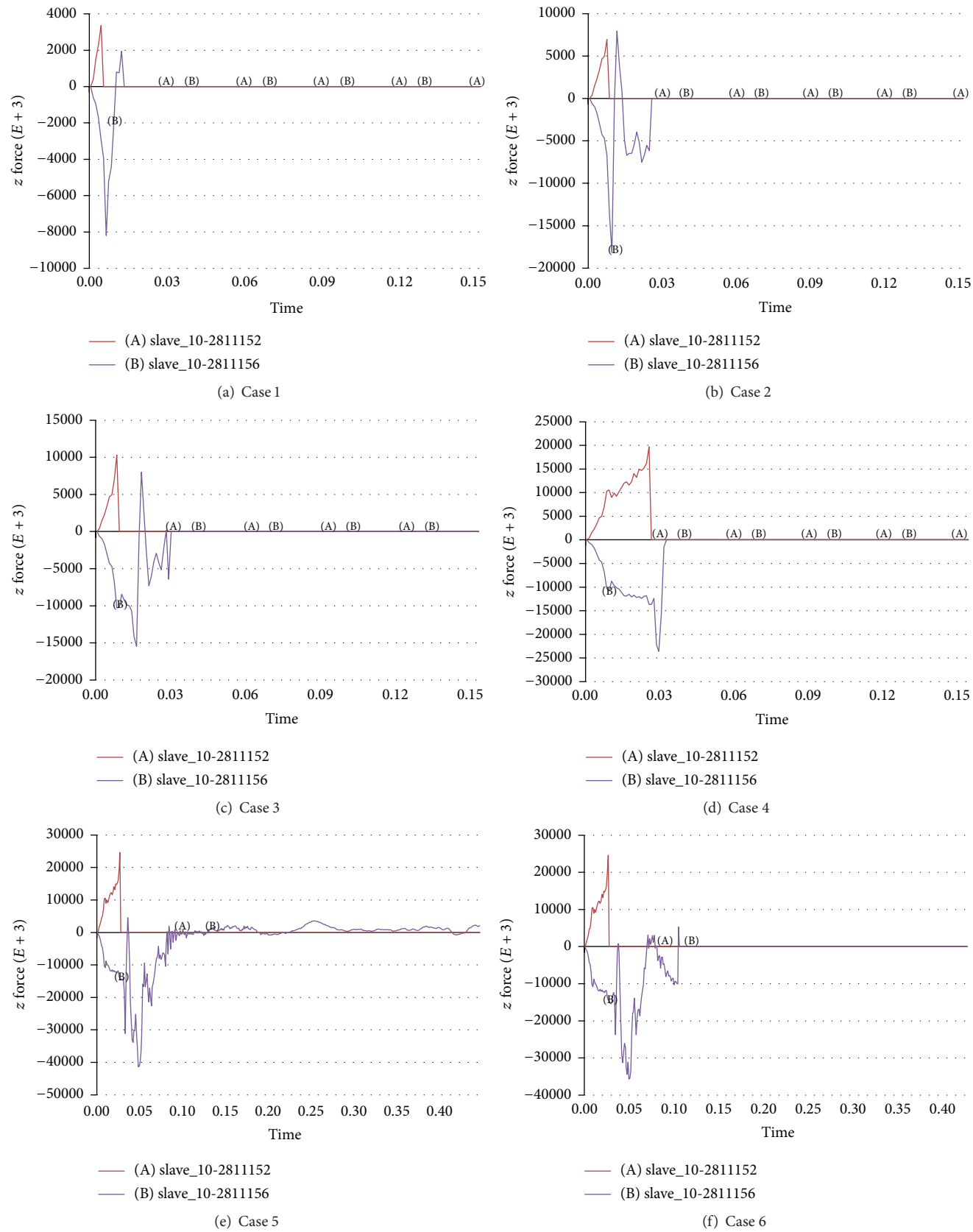

Figure 12: Continued.

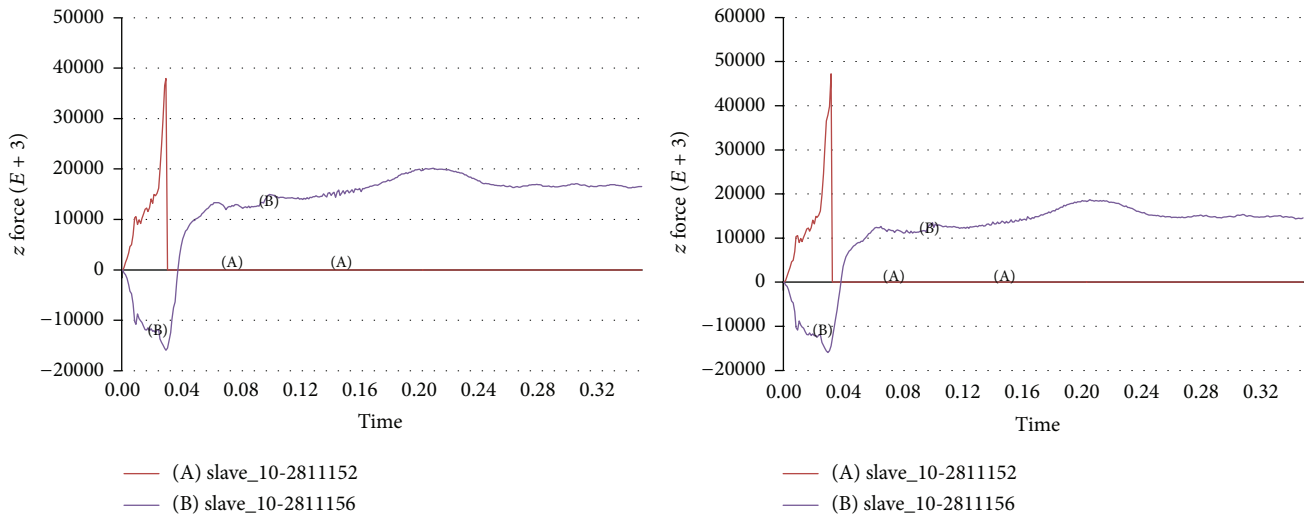

(g) Case 7 (h) Case 8

Figure 12: Induced vertical forces in the z-axis at the point of failure force measurement (cases 1~8).

Table 1: Analysis cases by different breakaway conditions ($f_{t\text{-max}}$ (N)).

SS400	Case 1	Case 2	Case 3	Case 4	Case 5	Case 6	Case 7	Case 8
	5,000	10,000	15,000	20,000	25,000	30,000	40,000	50,000
SM490	Case 9	Case 10	Case 11	Case 12	Case 13	Case 14	Case 15	Case 16
	5,000	10,000	15,000	20,000	25,000	30,000	40,000	50,000

Figure 11 shows the z-axis vertical forces obtained at the two nodes when the posts built with SS400 and SM490 are in full contact. The vertical force over time is higher with the B node compared to the A node. In the cases with SS400, the value rose up to 67,200 N, while the values in the SM490 scenario rose up to 677,000 N. With the maximum vertical forces of these graphs as the starting point, we performed simulations for the failure forces presented in Table 1.

4.2. Case II: Breakaway-Type Posts. The interpretations of each case in accordance with the breakaway conditions in (1) are shown in Table 1. Table 1 shows the different contact conditions between the detached posts. The contact conditions are defined to the maximum vertical forces at the time of the breakaway. Each force is determined from results for the full contact as shown in Figure 11.

Figures 12(a)–12(h) show the induced vertical forces at the A and B nodes for SS400. Based on the failure conditions of each case, the induced vertical forces are shown to be within the failure force range. As the failure force increased, breakaway at A node occurred as expected, while the B node showed an increase from the compression force to the tensile force. Such a phenomenon can be observed in cases 7 and 8. The results of the simulation indicate that the posts are still upright after the crash. That is, the breakage at A node happens from case 7 on, but at B node, the breakage never occurs.

Figures 13(a)–13(h) show induced vertical forces at A and B nodes for SM490. While the graph shows a similar tendency with that of the SS400 material, the overall vertical force is higher. However, from case 14, there is a vertical force generated at the B node that prevents the post from breaking away. This indicates a failure force condition of 30,000 N, which is lower than the failure force condition of case 7 for SS400, which was 40,000 N. We may conclude from these results that this is because of the increased physical strength of the post due to using a material of higher strength, causing more tensile force to the breakaway base of the post. In summary, the threshold of breakaway for SM490 is lower than that of SS400.

Figures 14-15 show the deformed shapes of the breakaway-type post and car against the crash for different cases. As expected, it can be observed from figures that posts made of SM490 are not breakaway or less deformed when compared to SS490 for the same failure condition because of the increased stiffness.

4.3. Case III: Passenger Safety Performance Assessment. Figures 16-17 show induced THIV and PHD for measuring the vehicles acceleration in x-, y-, and z-axis as well as the rotational velocity [15]. Assessments of the THIV and PHD are performed based on the passenger safety performance assessment items [11]. In the case of THIV, passenger safety could be guaranteed when the speed is 33 km/h.

The passenger car models were built based on the models provided by NCAC. We followed the guidelines (SB2 and

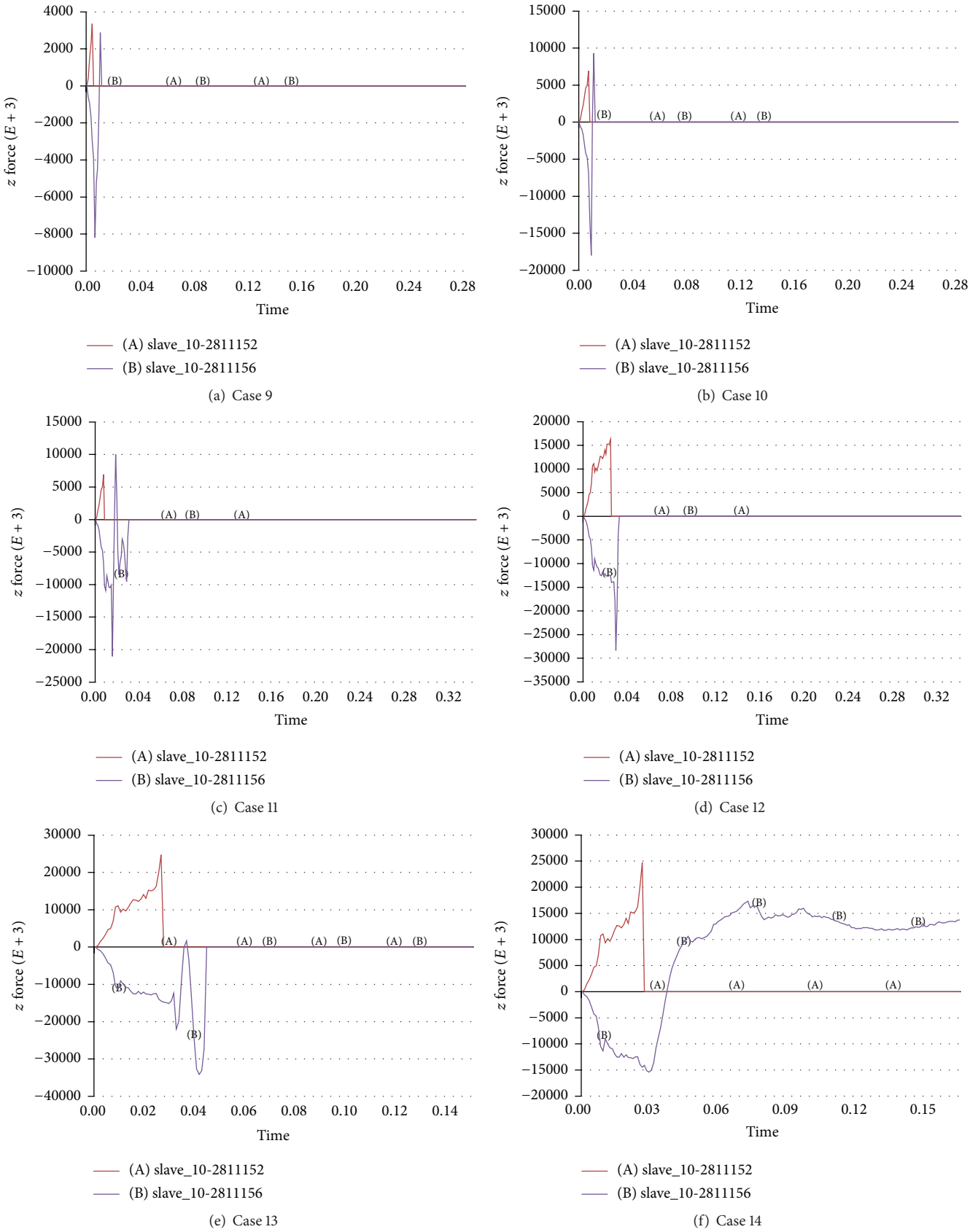

Figure 13: Continued.

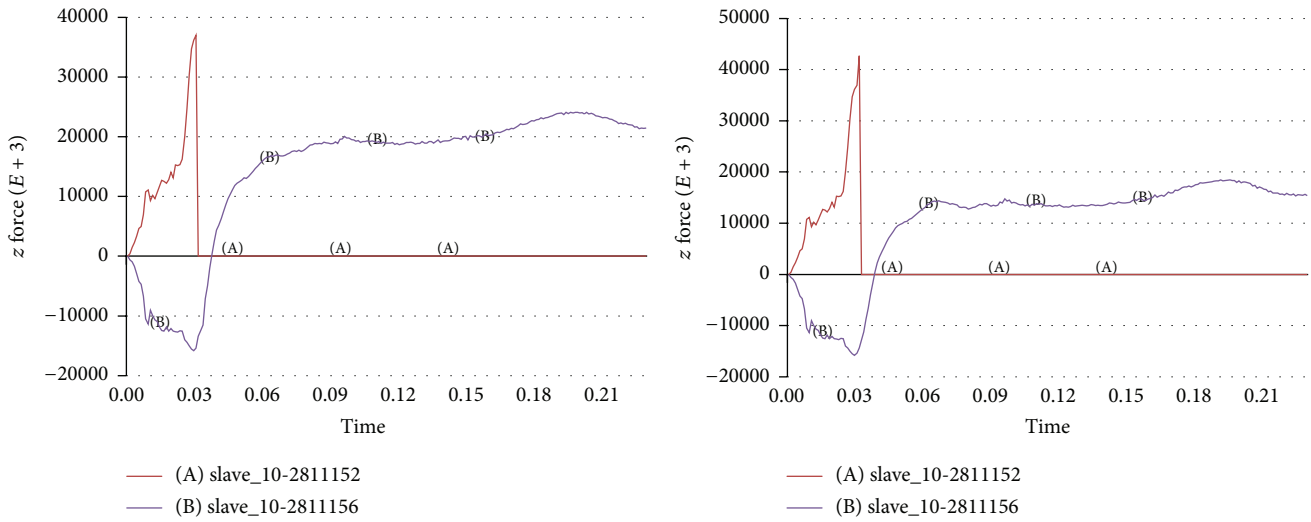

(g) Case 15 (h) Case 16

Figure 13: Induced vertical forces in the z-axis at the point of failure force measurement (cases 9~16, SM490).

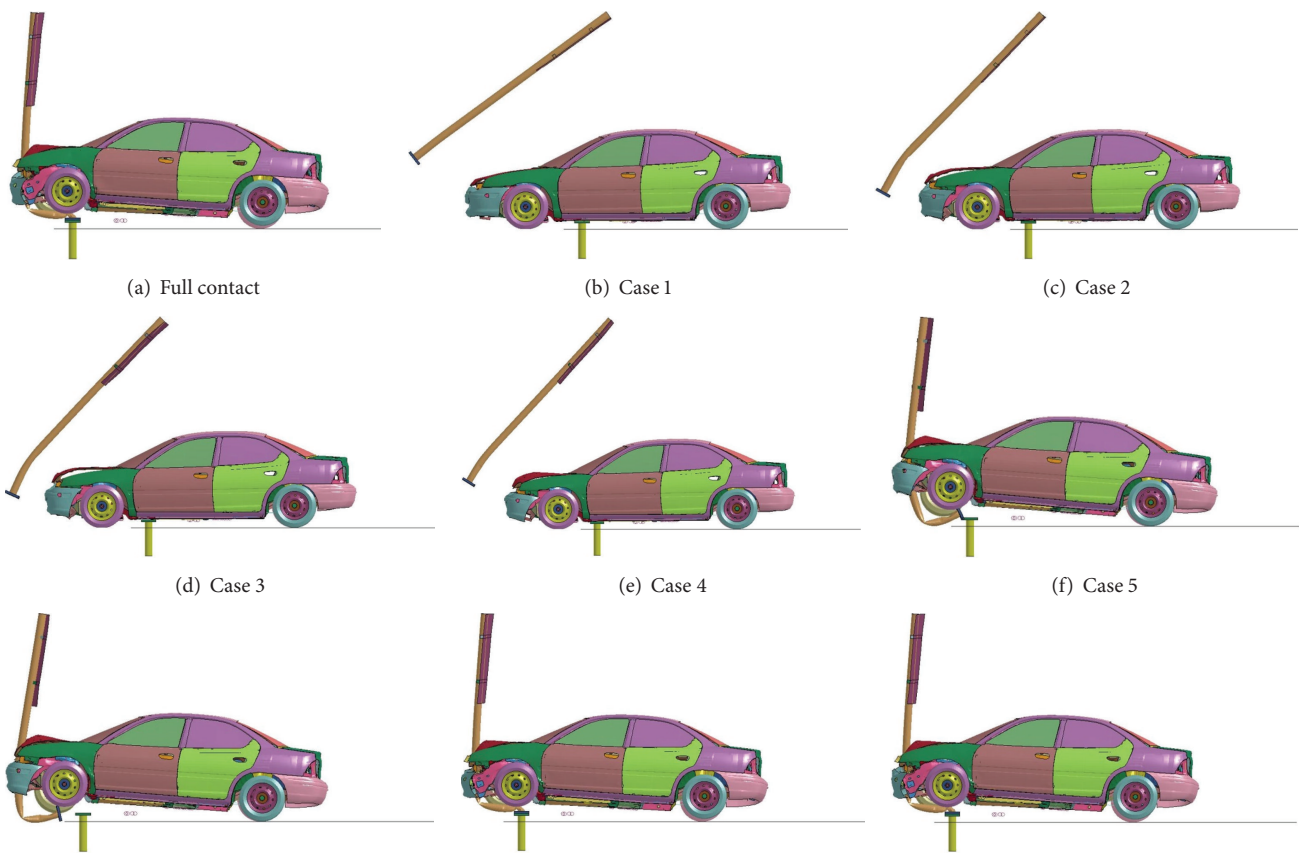

(a) Full contact (b) Case 1 (c) Case 2

(d) Case 3 (e) Case 4 (f) Case 5

(g) Case 6 (h) Case 7 (i) Case 8

Figure 14: Deformed shapes for different cases (SS400).

SB4 grades) to test the rails in Korea as per the Guideline to Perform Crash Tests for Road Side Barriers [16]. In the SB2 and SB4 grade regulation, the mass of impact vehicle is 900 kg and impact speed is 80 km/h. In this study, the requirement is satisfied for both SS400 and SM490, within the failure force range of 40,000 N. However, in the case of PHD, the SS400 satisfied the requirement under 50,000 N, while SM490 does so under 40,000 N. If we relate this to the breakage results

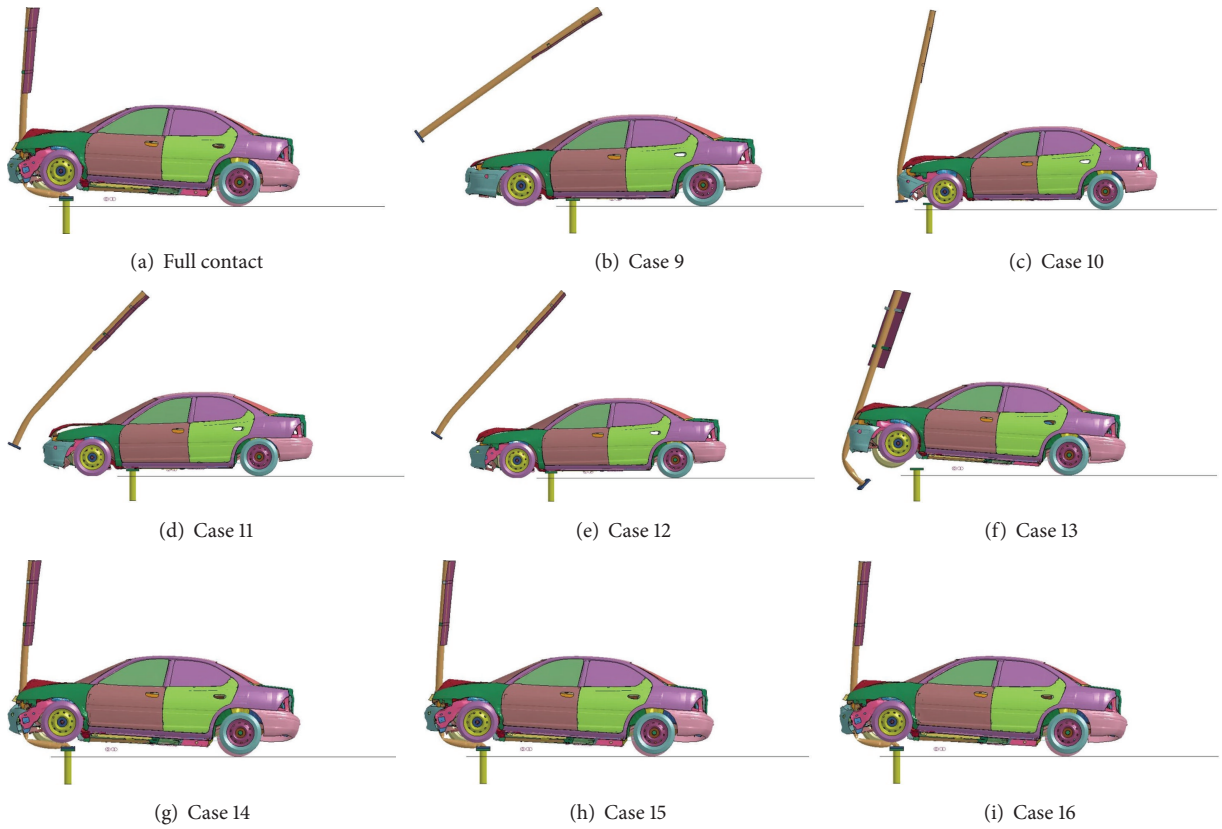

Figure 15: Deformed shapes for different cases (SM490).

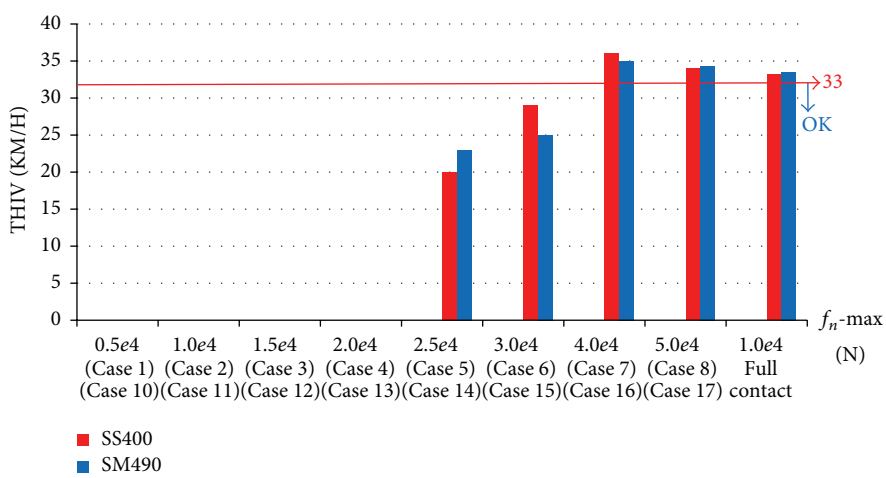

Figure 16: THIV for different cases.

discussed earlier, the SS400 is believed to have satisfied the THIV requirement after the breakaway, while SS490 satisfied the THIV requirement in case 14, where the breakaway did not occur. The same is true with the PHD. In other words, the condition that both THIV and PHD should be satisfied for SS400 and SM490 is that the failure force is lower than 40,000 N.

5. Conclusion

In this study, we performed the assessment of passenger safety for posts and signboards that are standard roadside installations. To disperse the impact force when a car crashes into a post, the post is designed with a breakaway feature. The simulation is performed with two different materials: normal

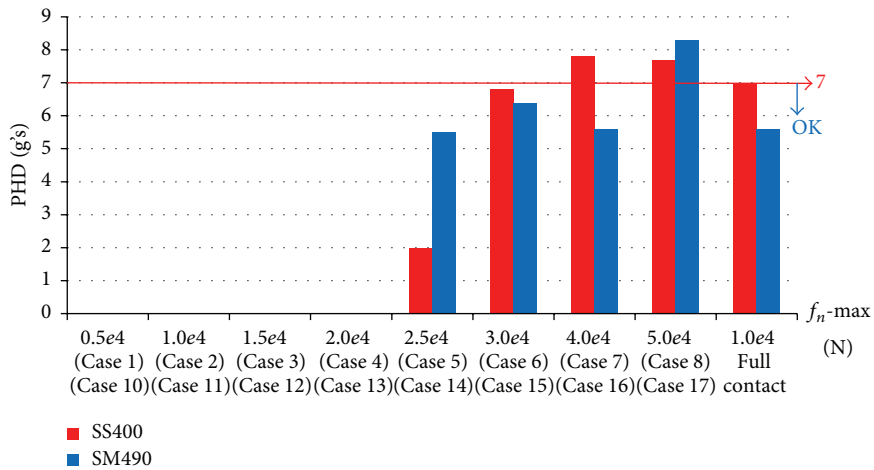

Figure 17: PHD for different cases.

steel (SS400) and high anticorrosion material (SM490.) We determined that previous studies did not provide sufficient explanations of the mechanism of breakaways. Therefore, this study is performed to clarify the conditions of post breakaway. The simulation was carried out using LS-DYNA and the TIEDBREAK_NODES_ONLY option, which considers the failure force between the nodes at the post base. We assumed a full contact condition between the posts and calculated the vertical force over time after the impact under this initial condition. Then, with the maximum vertical force as the basis, eighteen cases are considered. The results show that the SS400 material has a higher breakaway requirement compared to that of SM490. Then this suggests that such difference is related to the physical properties of the steel material used for the post.

The assessment results of the passenger safety for THIV and PHD show that the requirement is satisfied under 40,000 N for both the SS400 and SM490 materials. However, in the case of SM490, while the post was not detached, both the THIV and PHD represent satisfactory results. In this study, we consider momentum to be a dominant factor for the failure and considered the vertical forces only. However, future studies that consider the shearing force as well could contribute to the enhancement of the results of the safety assessment. It will be also necessary to extend the concept from further studies for the wind resistance.

Competing Interests

The author declares that there is no conflict of interests regarding the publication of this paper.

Acknowledgments

This work was supported by the National Research Foundation of Korea (NRF) grant funded by the Korea government (MSIP) (no. 2015R1A2A2A01005637).

References

[1] G. R. Johnson and W. H. Cook, "Fracture characteristics of three metals subjected to various strains, strain rates, temperatures and pressures," *Engineering Fracture Mechanics*, vol. 21, no. 1, pp. 31–48, 1985.

[2] M. G. Ko, K. D. Kim, K. J. Kim, J. G. Sung, and D. G. Yun, "Study on the hazardousness of a rigidly connected circular post and crash worthiness of a circular post with release mechanism for head-on impacts using impact simulation," *Journal of the Korean Society of Road Engineers*, vol. 12, no. 4, pp. 197–202, 2010.

[3] W. Pawlus, K. G. Robbersmyr, and H. R. Karimi, "Mathematical modeling and parameters estimation of a car crash using data-based regressive model approach," *Applied Mathematical Modelling*, vol. 35, no. 10, pp. 5091–5107, 2011.

[4] G.-D. Kim and S.-Y. Lee, "Finite element crash analysis of support structures made of various composite materials," *Journal of Korean Society for Advanced Composite Structures*, vol. 6, no. 1, pp. 45–50, 2015.

[5] C. Liu, X. Song, and J. Wang, "Simulation analysis of car front collision based on LS-DYNA and hyper works," *Journal of Transportation Technologies*, vol. 4, pp. 337–342, 2014.

[6] Y. Zhou, F. Lan, and J. Chen, "Crashworthiness research on S-shaped front rails made of steelaluminum hybrid materials," *Thin-Walled Structures*, vol. 49, no. 2, pp. 291–297, 2011.

[7] Y. Zhang, G. Sun, G. Li, Z. Luo, and Q. Li, "Optimization of foam-filled bitubal structures for crashworthiness criteria," *Materials and Design*, vol. 38, pp. 99–109, 2012.

[8] J. Choung, W. Nam, and J.-Y. Lee, "Dynamic hardening behaviors of various marine structural steels considering dependencies on strain rate and temperature," *Marine Structures*, vol. 32, pp. 49–67, 2013.

[9] G. Cowper and P. Symonds, "Strain hardening and strain rate effects in the loading of cantilever beams," Brown University Applied Mathematics Report 28, 1957.

[10] M. A. Crisfield, *Nonlinear Finite Element Analysis of Solids and Structures*, John Wiley & Sons, 1997.

[11] AASHTO, *Manual for Assessing Safety Hardware*, AASHTO, 2009.

[12] ANSYS Corp, *ANSYS(LS-DYNA) User's Manual*, ANSYS Corp, 2012.

[13] J. E. Bowels, *Foundation Analysis and Design*, McGraw-Hill, New York, NY, USA, 2nd edition, 1977.

[14] National Crash Analysis Center (NCAC), 2000, http://www.ncac.gwu.edu/ncac/.

[15] Test Risk Assessment Program (TRAP) Version 2.0 User's Manual, 1999.

[16] Ministry of Land, Infrastructure and Transport (MLIT), Guideline to Perform Crash Tests for Road Side Barriers, 2012 (Korean).